C_{60} single domain growth on indium phosphide and its reaction with atomic hydrogen

M. Eremtchenko, S. Döring, R. Temirov, and J. A. Schaefer*
Institut für Physik und Zentrum für Mikro- und Nanotechnologien, Technische Universität Ilmenau, P.O. Box 100565, D-98684 Ilmenau, Germany
(Received 15 July 2004; revised manuscript received 15 October 2004; published 11 January 2005)

The growth of C_{60} fullerene films on InP(001)-(2×4) was studied under ultrahigh vacuum conditions. The spectral signature of the C_{60} films was measured using high resolution electron energy-loss spectroscopy. Our data show that the molecules are bonded weakly to the substrate, leading to three-dimensional (3D) cluster formation of C_{60} at the initial stages of deposition. This is indicated by spectroscopic and microscopic observations. Surprisingly, low-energy electron diffraction and scanning tunneling microscopy measurements reveal that further molecule deposition forms a well ordered single domain film. From the analysis of our microscopic data, we have determined that the C_{60} film has an fcc (111) orientation. The influence of structural inhomogeneities and indium clusters, which are the most prevalent defects of the InP(001)-(2×4) surface, on the molecular film properties was studied. A shift of the substrate carrier plasmon under annealing was detected. The stability of the C_{60} film under exposure to atomic hydrogen was investigated. High reactivity of the molecules was detected. Further exposure does not change the surface, which indicates the formation of a stable coverage by the chemical modification.

DOI: 10.1103/PhysRevB.71.045410 PACS number(s): 81.05.Tp, 68.37.Ef, 68.43.Pq, 68.55.Ac

I. INTRODUCTION

Since their discovery, caged carbon structures[1,2] have attracted much scientific interest. Strong research activities in the field are stimulated by the promising properties of fullerenes. The *n*-type conductivity of the C_{60} fullerenes[3] excites an interest in its incorporation into electronic technology. The design of electronic devices is one possible application of these materials.[4–6] For most technological applications based on thin molecular films the key problem is the formation of homogeneously ordered structures, because the defect density is crucial for the performance of devices.[7,8] From this point of view, the search for complementary materials and growth parameters, which allow the manufacturing of well ordered molecular structures, is a very relevant topic. This problem has stimulated a great number of investigations related to fullerene structures on semiconductors.[9–15] C_{60} growth on gallium arsenide[9] or clean[10] and hydrogenated[11–13] silicon was studied in great detail. Indium phosphide as a substrate for the formation of C_{60} films has not received large attention yet, in contrast to some other semiconductor surfaces. Only two studies of C_{60}/InP have been reported, a spectroscopic study by Chao *et al.*[14] and the paper by Dmitruk *et al.*[15]

Due to the investigations of the fullerene films grown on indium phosphide substrates is at the very beginning, the technological applications of this structures have not been developed yet. Here we only refer to the possible applications of C_{60} for molecular field-effect transistors and solar cells, where thin InP films could serve as templates of the well ordered molecular films. A more detailed discussion about possible applications of the particular C_{60}/InP structures for device production is beyond the scope of this paper.

In this contribution we present spectroscopic and structural investigations of C_{60} growth on InP(001). The good correspondence of the C_{60} diameter (0.71 nm, which corresponds to a 0.87 nm intermolecular distance in a close packed lattice[2,16]) with the unit cell dimensions of the (2×4) reconstructed InP(001) surface $(0.83\times1.66\ \mathrm{nm}^2)$,[17–19] makes this substrate very promising for the growth of commensurate close packed fullerene overlayers. Remarkably, the single domain molecular film formation we registered by both STM and LEED, which could be interesting for the development of a technique for fullerene crystal growth. The molecular layers formation is strongly dependent on interface interactions. Strongly interacting substrates usually limit the molecular mobility along the substrate during film formation, thus leading to the appearance of grains; whereas weakly interacting interfaces in many cases lead to island formation on the substrate. Therefore, the molecule-substrate interaction plays an important role in the film growth process and was studied in this work by spectroscopic techniques. The data are important for the discussion of the mentioned remarkable C_{60} structure formation.

For technological applications the stability of the growth mode with respect to the density of common substrate defects is an important question. Reproducibility of the structures at various conditions can restrict possible applications of these materials and therefore the influence of defects on the molecular film growth attracts much interest. The InP(001)-(2×4) surface reconstruction is obtained by phosphorus depletion during substrate heating,[20–23] which may also lead to the formation of indium clusters on the surface. The metallic indium clusters are normally the most frequent defects of this reconstructed surface. We have studied the influence of these metal clusters on the growth of C_{60} multilayers.

The last part of our contribution is related to the formation of a stable passivating film of the C_{60} structures. Manufacturing of electronic devices is often related to various chemical treatments and influences of environmental factors which strongly decrease the performance of the devices. As re-

ported in Ref. 5 and 6, the main problem of thin-film transistors based on C_{60} structures is their instability under atmospheric conditions. The penetration of contaminants can be related to the fullerene activity with respect to the attachment of radicals in solution or gas phase, as well as to a simple embedding in the molecular structure. This problem stimulates interest into the chemical activity of fullerene structures and the production of protective layers in order to avoid the destruction of the films. For example, alumina coverage was studied in Ref. 24. Protective films can also be produced by a surface reaction of C_{60} with atomic hydrogen. This reaction has been studied previously.[25–27] Also, C_{60} film annealing or *e*-beam bombardment result in reactions with hydrogen from the residual gas. Corresponding products were studied in Refs. 11 and 13. However, attention was mainly attracted to hydrogenated fullerene $C_{60}H_n$ formation, while in our experiments the emphasis is in molecule cage cracking and the properties of the products, which could serve as a protective layer for fullerene film against degradation in ambient conditions.

II. EXPERIMENT

The experiments were carried out in an ultrahigh vacuum (UHV) system equipped with an analytical chamber (base pressure of 4×10^{-11} mbar) and a preparation chamber (base pressure 3×10^{-10} mbar). The system includes a number of surface sensitive techniques: high resolution electron energy loss spectroscopy (HREELS), scanning tunneling microscopy (STM), x-ray photoelectron spectroscopy (XPS), ultraviolet photoelectron spectroscopy (UPS), and low-energy electron diffraction (LEED).

Spectroscopic properties were measured by a HREELS Delta 0.5 (developed by Ibach's group). The device allows measurement of vibrational spectra with a nominal resolution up to 8 cm^{-1} in straight-through geometry. Unfortunately, in reality, the sample has low scattered signal. Therefore, the resolution needs to be decreased in order to offer a drastically high signal. Also low-energy excitations such as phonons and plasmons broaden all spectral features.[28] In the case of InP surface satisfactory statistics reaches at a full width at half maximum (FWHM) of about 30 cm^{-1} of the elastic peak.

Both specular and off-specular regimes were exploited for registering dipole and impact active molecular vibrations, respectively.[28] For the precise analysis of peak positions the HREELS data were deconvoluted using Razor Library software with the implementation of the Richardson-Lucy maximum likelihood algorithm.[29] In the process of deconvolution the reduction of the spectrometer broadening was done by subtracting the instrument response function from the experimental data. The instrument response function was defined from the elastic peak of the measured spectrum. Because the accuracy of this procedure is limited, we also present the raw spectra for some curves. These data are shown where the principal peaks are rather weak in order to allow the reader to judge the applicability of the algorithm in these cases (see below).

For the characterization of the surface structure, STM (Omicron variable temperature STM) was used as a local probe. Micrographs of crystal substrates [InP(001), Si(111), Ag(111)] with atomic resolution were used for STM calibration. The long-range order was investigated by LEED (VSI ErLEED 1000-D).

In this work, XPS was mainly used to determine the thickness of the adsorbed film. The spectrometer was adjusted in these experiments such, that the full width at half maximum of core level peaks was 1.5–2.0 eV. The attenuation of the substrate peak intensities with respect to the adsorbate related features at different coverages allows us to calculate the molecular film thickness.[30] In order to achieve better accuracy, the method was preliminary applied to calibrate our C_{60} source. For this purpose an Ag(111) substrate was used, because the molecules form a film with homogeneous thickness on this substrate.[31,32] The evaluation of the XPS data (attenuation of the substrate core level Ag3*d* peak intensity at a binding energy $E_B=368$ eV with respect to the molecule related C1*s* intensity at $E_B=284$ eV) of consecutively deposited portions of C_{60} was used for the calibration of molecular source dosing. By using Ag(111) as a substrate, the calibration procedure can be verified by an alternative technique. The vibrational signature of the C_{60}/Ag(111) interface differs from a multilayer spectrum. The A_g Raman mode of C_{60} reveals itself in dipole spectra at 1445 cm^{-1} due to an interfacial dynamic charge transfer mechanism.[33–35] The mode is the most intensive for the coverage of 1 ML and this effect allows confirmation of the film thickness values measured by XPS by comparison with the corresponding HREEL spectra. In addition to the preliminary molecular source calibration the film thicknesses of C_{60}/InP(001) structures were also evaluated from the XPS data. In this case the attenuation of the In3*d* peak ($E_B=444.5$ eV) with respect to the C1*s* peak was determined. The obtained values correspond reasonably well (±25%) to those expected from source calibration.

A hot capillary source of atomic hydrogen was employed for the surface treatment. The device provides much more efficiency than the well known hot filament technique.[36] This technique allows a decrease in the exposition time and therefore a decrease in the surface contaminations by residuals and heating during the procedure. The outer part of our atomic hydrogen source is well shielded by a closed water cycle, the outer window in the cooled shell has a diameter of about 3 mm. The distance between sample and local source was about 8 cm. Nevertheless the temperature was not monitored during the treatment, taking into account short exposition time, cooled shield and small aperture of the atomic hydrogen source we would not expect a significant increase of the sample temperature. For the quantitative estimation of the atomic hydrogen dosing we take into account the H_2 gas pressure in the UHV chamber and the exposure time [1 Langmuir (L) $=10^{-6}$ Torr $\times$ s] with respect to the hot filament technique.

C_{60} was deposited from a Knudsen cell. The source was degassed by heating at 600 K for about 20 h before deposition of the molecular film. A deposition rate of 0.25 ML/min at a source temperature of 670 K was used. During the evaporation the sample was kept at room temperature with negligible increase due to a distance of about 25 cm between sample and shielded local heater.

InP(001) substrates were from MCP Wafer Technology, Ltd. and Crystec, GmbH. Undoped samples with an intrinsic carrier concentration lower than 10^{16} cm^{-3} and S doped with a carrier concentration of 10^{19} cm^{-3} and 2×10^{18} cm^{-3} were used. The frequencies of the carrier plasmon for the doped samples are 760 and 407 cm^{-1}, respectively, due to the carrier plasmon energy depending on the dopant concentration. The clean InP(001) surface was prepared similarly to earlier studies.[20–23] At first, InP was etched in 40% HF for 30 s, then rinsed in distilled water. The samples were preliminary heated at about 370 K for 10 h in order to remove surface contaminations. Gentle sputtering by Ar ions at an energy of 0.5 keV for 6 min with a sample current density 1 $\mu A/cm^2$ at an ion beam angle plus and minus 45° with respect to the sample normal was used as the next cleaning step. Formation of InP(001)-(2×4) was completed by substrate heating up to 670 K for 5 min.

III. RESULTS AND DISCUSSION

A. Interface interactions

In this paper the discussion of the spectroscopic properties of C_{60} films on InP(001) precedes structural studies in order to clarify the interaction picture at the molecule-substrate interface. Data obtained at various coverages were compared to study the interface spectral features. The response from the interface can be registered at about 1 ML coverage, whereas this signal is attenuated at higher film thicknesses, and at about 10 ML only bulk properties of the film are studied.

Initially, XPS peak positions and shapes were carefully measured for various coverages in order to study the chemical interaction of C_{60} with InP. Chemical bonding in most cases causes energy shifts of the core levels of interacting species, then the lines of corresponding core levels should be shifted. In our experiments such shifts were not registered in contrast to Ref. 14. Note, that due to inhomogeneities of the film structure at nominal coverages of about 1 ML (see below), slightly shifted substrate components from areas covered by C_{60} could be hidden by nonshifted components from the clean substrate. Even regarding this effect, only weak bonding could follow from our measurements. Moreover, predominant C_{60} bonding to indium or phosphorus was not detected in our experiments.

The interfacial interaction is also revealed in the vibronic spectra. In case of specific bonding to the substrate the vibrational frequencies of molecules at the first monolayer are shifted with respect to the multilayer spectrum. A set of deconvoluted vibronic HREEL spectra of C_{60}/InP(001) is presented in Fig. 1. The peaks related to InP(001) are present in all spectra, also the vibration signature of clean InP(001) is shown in (a) as a reference. The Fuchs-Kliewer (FK) optical phonon at 339 cm^{-1} and its double loss dominate the spectrum.[20,22] The broad peak related to the carrier plasmon (CP) is centered at 760 cm^{-1} (the carrier concentration in this case was 10^{19} cm^{-3}). The plasmon energy is sensitive to surface treatment and is discussed in detail below (see e.g., Ref. 20).

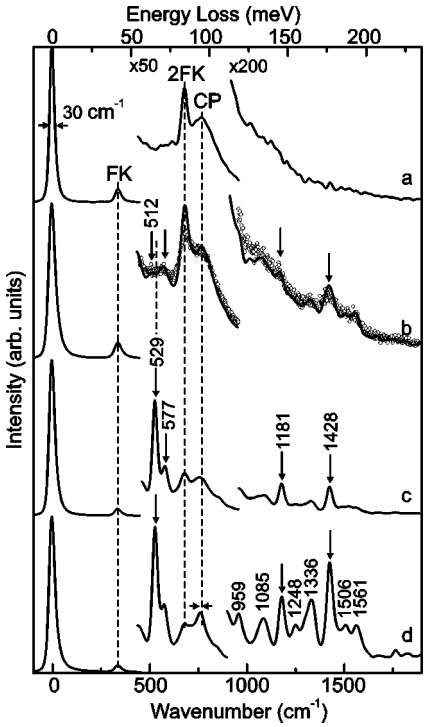

FIG. 1. HREEL spectra of C_{60}/InP(001)-(2×4) (primary beam energy 4.5 eV, incident angle 64° with respect to surface normal). Magnified parts of the spectra are deconvoluted, the raw spectrum is depicted by open circles (see text). (a) Clean InP(001), (b) 1 ML C_{60}, and (c) 10 ML, in the specular regime; (d) 10 ML, off specular (6.9°). The four molecular dipole active T_{1u} modes, Fuchs-Kliewer phonon (FK, 2FK), carrier plasmon (CP), and its imaginary shift are marked (see text). Only one molecular vibrational line (529 cm^{-1}) is shifted in the interface spectrum with respect to C_{60} bulk.

The spectra of the C_{60} monolayer and multilayer measured in specular geometry are shown in Fig. 1 (b,c), respectively. Because only the dipole active modes are registered in specular geometry, the response from C_{60} in these curves consists of four peaks (indicated by arrows) which correspond to the well known T_{1u} vibrations of C_{60}.[37–42] These modes become stronger in the multilayer spectra. These dipole active modes at 529, 577, 1181, and 1428 cm^{-1} are well resolved in spectrum (c) and their positions fit to previously reported experimental[37,38,41,42] and calculated[39,40] data. The measured HREELS peak positions coincide with accuracy less than 5 cm^{-1} (see Table I) to the reported optical spectroscopy data, which are the most accurate among the vibrational spectroscopy techniques. In spectrum (b) these modes are also registered (the peak at 1181 cm^{-1} is not strongly pronounced in this curve due to the weakness of the signal). It is important that the first T_{1u} mode is shifted to 512 cm^{-1} in the monolayer spectrum, while all other peaks are at the same positions within experimental accuracy (about 5 cm^{-1}). Also the relative peak intensities changed due to the interface interaction. Note that C_{60} deposition leads to 3D cluster formation even at low coverages (see below) and the spectral features of the interface are slightly distorted already at submonolayer coverages. This effect decreases the accuracy and makes the spectral analysis more complicated.

TABLE I. C_{60} vibration frequencies (cm^{-1}) measured by HREEL, infrared and Raman spectroscopies in comparison with calculated values (see text). Dipole active modes are marked by bold faced numbers.

HREELS (this work)	HREELS (Ref. 41)	IRS (Ref. 37)	Raman (Ref. 42)	Calcul. (Ref. 39)	Calcul. (Ref. 40)
529	**532**	**527**	**533**	**547**	**528**
577		**579**	**580**	**578**	**595**
959	968	962	962	994	989
1085	1097	1100	1080	1153	1123
1181		**1183**	**1187**	**1208**	**1222**
1248	1258	1259	1251	1250	1288
1336		1330	1346	1396	1337
1428		**1429**		**1445**	**1489**
1506		1502	1502	1534	1538
1561	1565	1571	1577	1575	1609

The relations between the vibrational frequency shifts and the charge transfer were carefully studied for structures such as C_{60} doped with alkali metals and adsorbed on metal substrates.[43–45] There is an almost linear dependence of the peak shift due to a charge transfer, namely, $-10.1\ cm^{-1}$ per electron for the $T_{1u}(1)$ mode and $-14.5\ cm^{-1}$ per electron for the $T_{1u}(4)$ mode, while the $T_{1u}(2,3)$ are almost not sensitive to charge transfer.[43] At the same time, a distortion of molecules at the interface can modify this behavior. The $C_{60}/InP(100)$-(2×4) interface shows a shift of about $17\ cm^{-1}$ only for the $T_{1u}(1)$ mode, this value is lower than for the weakly interacting substrates such as metals, compare, e.g., a redshift of $24\ cm^{-1}$ for noble metal substrates and $32\ cm^{-1}$ for Ni(110).[43] This shift reveals the existence of a distortion of the molecule at the interface, but this effect is weak, which is expected because the In-rich substrate is electron deficient and therefore almost no large charge transfer is possible. The weakness of the C_{60} distortion at the interface confirms that the bonding between C_{60} and InP(001)-(2×4) is not strong if compared to metals, for example. This conclusion is in general agreement with the Raman spectroscopy data of C_{60} deposited on the unreconstructed InP(001) surface.[15]

A number of dipole nonactive modes excited by impact scattering are resolved additionally in the off-specular spectrum, as shown in Fig. 1(d). The measured peak positions are presented and compared with referred data in Table I. All molecular vibration energies correspond to previously reported peaks of HREEL,[41] infrared,[37,38] Raman[42] spectroscopic, and calculated[39,40] data. A few molecular vibrations below $800\ cm^{-1}$ are hidden by the substrate peaks. For example, the peak at about $760\ cm^{-1}$ fits to the carrier plasmon position, and the resulting plasmon frequency seems to be slightly shifted in the off-specular spectra [Fig. 1(d)]. The spectral signature of the real molecular structure of C_{60} at the interface is characterized by the appearance of mode combinations and the same frequencies could be related to various vibrations or their combinations. Detailed analysis of electron energy loss peak intensities with respect to excitation mechanisms can shed light on this problem, but this is not included in this contribution.

It is important to note in this paper that the large ratio between infrared and Raman mode intensities in the dipole spectra measured by HREELS points to the well ordered surface. This is related to the effect reported by Lucas.[46] Increased surface disorder results in a broadening in angle of the dipole lobe, where electrons scattered by the dipole mechanism (infrared active modes) are focused. At the same time, the angle distribution of the electrons scattered by the impact mechanism (Raman active modes) is not sharp and not strongly affected by the surface order. Therefore, the better the long-range order in the film, the higher the intensity of the infrared active modes relative to the Raman active modes. For the C_{60} films the intensity ratio between $T_{1u}(1)$ and Raman losses at 529 and $760\ cm^{-1}$, respectively, serves to characterize the surface ordering. The highest reported ratio was up to 23 for well ordered films deposited on GeS (Ref. 47) and between 11 and 15 for layers on hydrogen terminated silicon (see, for example, Ref. 11). In the spectra presented in Fig. 1, the mode at $760\ cm^{-1}$ is obscured by the surface carrier plasmon loss. Thus it is more convenient to analyze this Raman peak in the spectra of Fig. 2, where the plasmon is shifted due to higher carrier concentration of the substrate. Inspecting Fig. 2(d), the estimated $T_{1u}(1)$/Raman intensity ratio is about 20, which indicates the high molecular order of $C_{60}/InP(001)$ films.

B. Carrier transfer at the interface

As was noted, the carrier plasmon position and intensity is sensitive to the surface treatment. In our experiments C_{60} adsorption on clean InP does not change the plasmon energy (see Fig. 1), but the excitation is strongly damped in the case of a thick adsorbate layer [curves (c) and (d)]. So, the molecules do not change the charge distribution at the semiconductor interface, which corresponds to the weak interaction between C_{60} and InP concluded in the previous section.

On the other hand, the formation of indium clusters by annealing[20–23] leads to a plasmon modification. In our experiments, the plasmon energy shifts from 815 to $925\ cm^{-1}$ and the intensity increases, as is shown in Fig. 2 [spectra (a) and (b)]. These changes could be related to the dopant drift

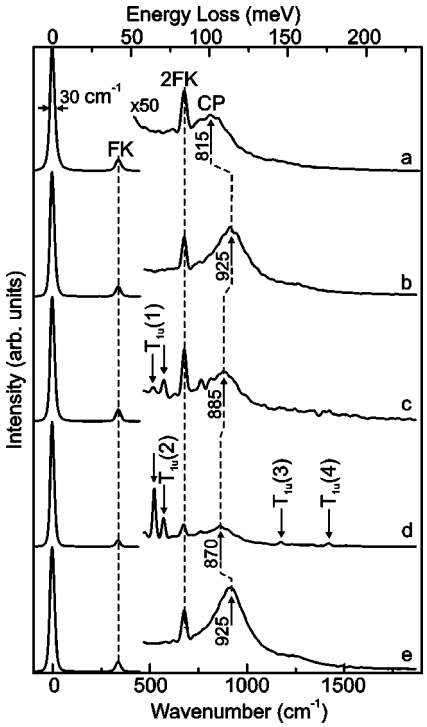

FIG. 2. HREEL spectra of C_{60}/InP(001)-(2×4) after consecutive surface treatment (specular regime, the same spectrometer settings as in Fig. 1). Magnified parts of the spectra are deconvoluted (see text). (a) Clean InP(001); (b) InP(001) annealed (5 min at 670 K) for In cluster formation; (c) 1 ML and (d) 10 ML of C_{60} deposited on the In-InP(001); (e) 10 ML C_{60} annealed (5 min at 650 K) for molecular layer removal. Carrier plasmon (CP), Fuchs-Kliewer phonon (FK, 2FK) and T_{1u} peak positions are marked (see text).

toward the surface during the heating procedure which apparently leads to an increase of the carrier concentration near the surface (detected by HREELS). The plasmon behavior could also be explained by a decrease of the depletion layer thickness by small metal clusters on the substrate. In this contribution we do not discuss this effect in detail. Note, that only on the modified surface, the C_{60} deposition leads to a decrease of the carrier plasmon frequency from 925 to 885 cm^{-1} [curves (c) and (d)] in contrast to the clean InP substrate (see Fig. 1). The effect is reversible, removing the molecules from the surface by annealing restores the initial position of the carrier plasmon [curve (e), compare with (b)]. Some increase of the plasmon intensity after C_{60} removal is related with an increase of the indium cluster density, because the molecule desorption requires almost the same temperature as phosphorus evaporation (650 and 670 K, respectively).

The influence of C_{60} on the carrier plasmon position only after substrate annealing could also be related to dopant drift toward the surface, which in our case leads to the appearance of sulfur atoms on the substrate surface. C_{60} adsorption on the defects can strongly modify the density of surface states even if the concentration of these defects is relatively low. The resulting modification of the depletion layer thickness leads to the plasmon energy shift.

The plasmon behavior can also be related to a strong selective interaction of the fullerene only with metal clusters on the complex structure. It is well known that the interaction of C_{60} with metals leads to a charge transfer into the adsorbed molecules. This was reported for a number of metals such as copper, silver, gold, and nickel[31,33,34,43–45] and the same effect for indium is expected. Negatively charged molecules decrease the carrier concentration in areas around the borders of the metallic clusters. If this boundary is relatively spread (in other words, if the clusters are small, which corresponds to our STM data, see below), the interface effect can produce a significant influence on the average carrier concentration near the surface and may lead to the registered decrease of the carrier plasmon frequency. The influence of C_{60} to semiconductor properties is mediated by metal clusters. A detailed understanding of the effect requires additional quantitative studying, for example, calculation of the energy shift as a function of the amount of the transferred charge by means of dielectric theory, which is beyond the scope of this work.

C. Structural properties

One can expect 3D cluster growth of C_{60} on InP(001)-(2×4) as a consequence of the weak interaction at the interface. The Vollmer-Weber three-dimensional growth was reported in Refs. 14 and 15. Our XPS data analysis also indirectly points to this growth mode: Using a model of a homogeneous molecular layer at small coverages, the evaluation of the XPS spectra provides smaller film thicknesses than expected from the molecular source calibration. On one hand this could be related to different sticking coefficients of C_{60} to InP(001) and to our reference Ag(111) substrate. On the other hand, it could result from an island growth mode, where discrepancies between the model (see Sec. II) and the real structures lead to a decrease of the calculated thicknesses. Also, no molecular structure was registered by LEED at coverages of about 1 ML. Therefore, direct microscopic study is required.

STM micrographs of InP(001) after about 1 ML nominal dosing of C_{60} are shown in Fig. 3. The high mobility of fullerenes on the substrate allows them to form well ordered, close packed molecular structures during the initial stages of deposition [see image (a)]. At the same time the growth of 3D clusters is registered. The edges of molecular terraces on the flat substrate are marked by arrows in image (b). Distortions in the STM pictures appear due to a movement of molecules by the probe at the cluster boundaries. The high mobility of C_{60} corresponds to weak bonding to the substrate.

Further C_{60} deposition leads to a growth of molecular clusters. Under these conditions the process could lead to a formation of multidomain mosaic structures resulting from randomly distributed clusters. This may take place on amorphous substrates or in the case of negligible molecule-substrate interaction. In contrast, our LEED and STM data show that C_{60} forms a single domain multilayer on InP(001)-(2×4) with orientational correspondence between the substrate and the molecular structures. This remarkable well ordered layer in shown in Figs. 4 and 5(b), where STM

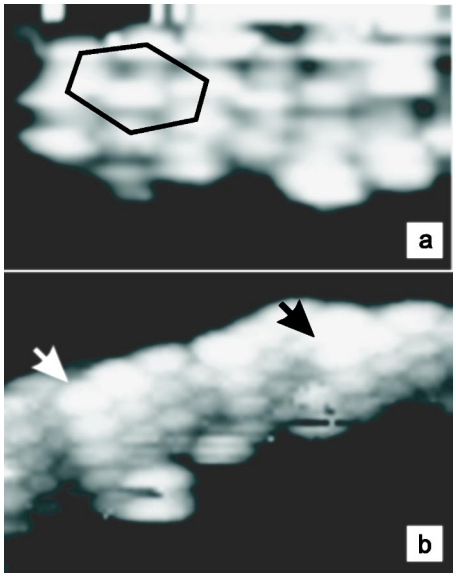

FIG. 3. STM micrographs of C_{60} clusters on InP(001) at 1 ML coverage. (a) 2D cluster (6×4 nm^2, $U_T=-3.2$ V, $I_T=0.1$ nA), close packed molecules are resolved (unit mesh is marked by a hexagon, an elongation in the horizontal direction is obviously related to the device drift), (b) 3D cluster (11×7 nm^2, $U_T=3.1$ V, $I_T=0.1$ nA), molecular terraces boundaries are marked by arrows.

and LEED images of a 10 ML C_{60}/InP(001) film are presented, respectively. Relatively large (in a range of a few thousand nm^2) flat terraces [Fig. 4(a)] are formed by well ordered molecules [Fig. 4(b)] with structures clearly resolved in high resolution images. Comparing the mutual displacement of the molecules in the neighboring terraces we have found an *ABC* structure of the C_{60} film. It corresponds to the well known fcc structure with (111) orientation.[2,16] Unfortunately, black-and-white representation does not allow to show with a good contrast the molecular lattices of a few terraces in one image, due to a large difference between the intermolecular corrugation depth (about 0.1 nm) and terrace steps (about 1.0 nm).

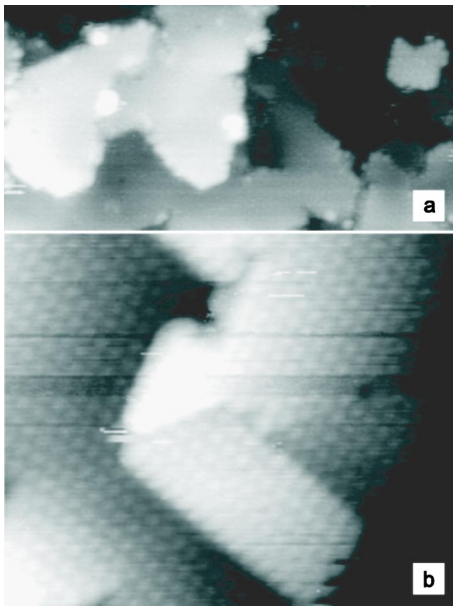

FIG. 4. STM micrographs of 10 ML C_{60}/InP(001). Terraces formed by the molecules at (a) moderate (75×35 nm^2, $U_T=3.1$ V, $I_T=96$ pA) and (b) high (25×20 nm^2, $U_T=3.1$ V, $I_T=96$ pA) resolution images are clearly resolved.

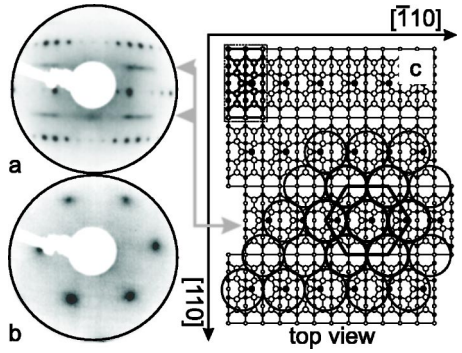

FIG. 5. Images of LEED patterns: (a) InP(001)-(2×4) (primary beam energy $E_0=70$ eV) shows the (2×4) reconstruction, smoothing of $\times2$ reflexes corresponds to structural defects marked in the drawing of this figure; (b) 10 ML of C_{60}/InP(001) ($E_0=12$ eV) shows single domain hexagonal molecular structure; (c) schematic drawing of C_{60}/InP(001)-(2×4). Substrate reconstruction is shown by small filled circles which correspond to P atoms, empty ones to In (the unit cell structure is presented in accordance with Refs. 17 and 18). The widespread shift of row of (2×4) unit cells [corresponding to the features of the LEED pattern (a), see text] is marked by the arrow. Arrangement of C_{60} is labeled by circles and the hexagon shows the molecular cell. Mutual disposition of the molecular rows with respect to the substrate grooves does not follow from our experimental data and is shown here only tentatively.

The orientation of molecular rows is the same on all terraces, which indicates a correlation between molecular and substrate ordering, but local probing by STM does not sufficiently prove long range surface order. The existence of the LEED pattern [see Fig. 5(b)] reveals long-range single domain order, while the hexagonal symmetry of the reflexes corresponds to our microscopic data. The comparison of substrate and adsorbate LEED patterns indicates that the C_{60} rows are parallel to the $[\bar{1}10]$ direction of the (2×4) reconstructed InP(001).

Nevertheless, intermolecular interaction dominates the structure formation, a correspondence between the substrate order and fullerene film growth is observed. The correlation leads to the formation of the single domain C_{60} adlayer, and the following growth model can be proposed. As was shown, small ordered molecular clusters appear at the initial stages of the deposition, and further growth forms 3D molecular islands. They merge in a single domain structure as if the initial small clusters were oriented and separated in a proper way. The order may only follow the substrate structure if the substrate parameters are appropriate and if the interaction with the adsorbate is strong enough. At the same time, the interface interaction should not restrict the adsorbate mobility. Due to a good correspondence of the parameters of the C_{60} fcc lattice (0.87 nm) and the (2×4) reconstructed InP(001) (0.83 nm), the molecules most likely fill the

grooves of the substrate surface[19] [see Fig. 5(a)], which play the role of a template for the initial cluster formation. The role of the substrate lattice period for the templating was confirmed by the following experiment. The (2×4) reconstruction was destroyed by the surface etching by atomic hydrogen, which leads to the formation of a (1×1) surface. The structure of the latter surface does not match the C_{60} fcc lattice, and the C_{60} deposition on this substrate under the same conditions does not form any molecular structure with long-range order. This observation is in accordance with Ref. 15, where the C_{60} clusters grow on the unreconstructed InP(001) surface prepared by washing in ethanol, de-ionized water and acetone. The correspondence of substrate and adsorbate dimensions together with the appropriate interaction strengths form the conditions for such an unusual growth mode of a single domain molecular structure.

D. Stability of the growth mode

Substrate defects are one of the most important limitations for the growth of high-quality molecular films. The formation of the (2×4) reconstruction by heating leads to a surface structure with two kinds of widespread defects: a breakage of the (2×4) periodicity and a metallic indium cluster formation. The appearance of these inhomogeneities always takes place and was registered by spectroscopic and microscopic techniques.

The first kind of substrate defects is related to the breakage of the periodicity in the [110] direction [see Fig. 5(c)], while the order in the $[\bar{1}10]$ direction is much better. This is directly visible in the LEED images of the substrate [Fig. 5(a)], where the (1×4) pattern is well resolved and the (2×4) order does not form clearly visible reflexes in reciprocal space (marked by the grey arrows in Fig. 5). In real space this defect may correspond to shifts of unit cell rows in the $[\bar{1}10]$ direction, which was registered by STM (see also Ref. 48). This kind of disorder does not destroy the grooves in the $[\bar{1}10]$ direction, which serve as a template for C_{60} ordering, and fortunately the molecular structure is not disturbed by the first kind of substrate disorder.

The second kind of InP(001)-(2×4) widespread defects is the appearance of metallic indium clusters. As was noted, the preparation of this substrate by heating is related to phosphorus evaporation and leads to an In-rich (2×4) reconstruction and simultaneous indium cluster formation. These two processes are coupled, and even the carefully prepared samples present some amount of metallic indium.[21] In order to register the influence of this kind of defect on the C_{60} layer formation, we increase the density of indium clusters by heating the sample to temperatures that are higher than necessary for preparation of a clean substrate (670 K instead of 650 K). The STM data show that annealing causes the appearance of objects with a very wide distribution of sizes (from about 10 to more than 500 nm) on the flat InP terraces which we relate to the clusters (see Fig. 6). Thus, the metallic indium droplets could possibly prevent the growth of a single domain molecular film in between these clusters. Our observations indicate that this does not take place. Deposition of

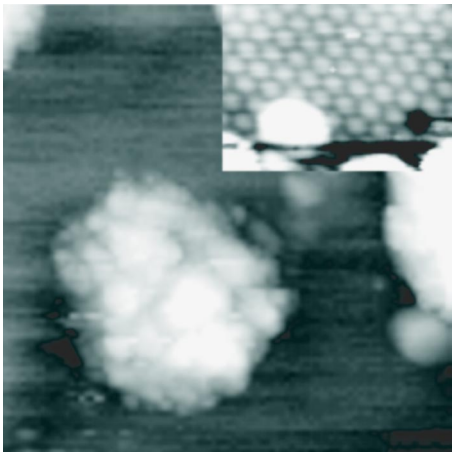

FIG. 6. STM micrograph of 10 ML C_{60} on annealed (5 min at 670 K) InP(001) (47×47 nm^2, $U_T=3.1$ V, $I_T=12$ nA) shows droplets on the flat terraces, which are related to metallic indium clusters. The high resolution image (inset) (11×8 nm^2, $U_T=4.5$ V, $I_T=0.15$ nA) of the terrace between the clusters indicates the existence of a well ordered molecular film.

C_{60} on the annealed substrate covered by indium clusters leads to the formation of the same structure as on the clean InP(001). The film still has a hexagonal LEED pattern, just the background becomes stronger. High resolution imaging shows a molecular structure between the defects, which likewise was registered on clean InP (see inset Fig. 6). Note, that the vibration signatures of C_{60} on InP(001) with and without the clusters are identical (compare the corresponding curves in Figs. 1 and 2), with the exception of the carrier plasmon modification (see above). The stability of the C_{60} growth mode with respect to widespread defects makes indium phosphide more attractive for possible applications in technology.

E. C_{60} etching by atomic hydrogen

In the Introduction the chemical instability of fullerene structures was mentioned. The problem induces, on one hand, the study of the chemical activity of the molecular structure with respect to different reagents and, on the other hand, the search for the protection of the C_{60} film.[24] In this work, we study the surface reaction of C_{60} with atomic hydrogen which can lead not only to fullerene hydrogenation but also to cage destruction.[11,13,25–27] The exposure to atomic hydrogen leads to drastic changes of the vibronic spectra, which we discuss in terms of a protective layer for the molecular structure.

The process of the molecular film hydrogenation is illustrated in Fig. 7. Curve (a) corresponds to the C_{60}/InP(001) multilayer, the fullerene signature [dipole active modes $T_{1u}(1)-T_{1u}(4)$] is marked by arrows. The intensities of the substrate features (FK, 2FK, and carrier plasmon at 407 cm^{-1}) are strongly damped by the molecular film, so the relative peak intensities allow us to monitor film thickness changes due to the surface treatment. Spectrum (b) was measured after only 2 L exposure of hydrogen. The appearance of bands at 1000–1500 cm^{-1} and 2800–3000 cm^{-1} corre-

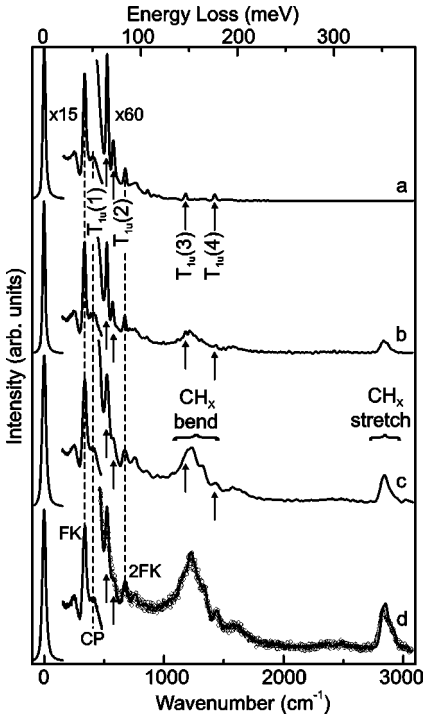

FIG. 7. HREEL spectra of C_{60}/InP(001)-(2×4) after atomic hydrogen exposure (primary beam energy 4.5 eV, incident angle 64° with respect to surface normal). Magnified (×60) parts of the spectra are deconvoluted, the raw spectrum is depicted by open circles (see text). (a) 20 ML C_{60}/InP(001); (b) the sample after 2 L hydrogen exposition (see text); (c) 6 L; and (d) 20 L. The C_{60} dipole active T_{1u} modes, substrate related carrier plasmon (CP) and Fuchs-Kliewer phonon (FK, 2FK) are marked (see text).

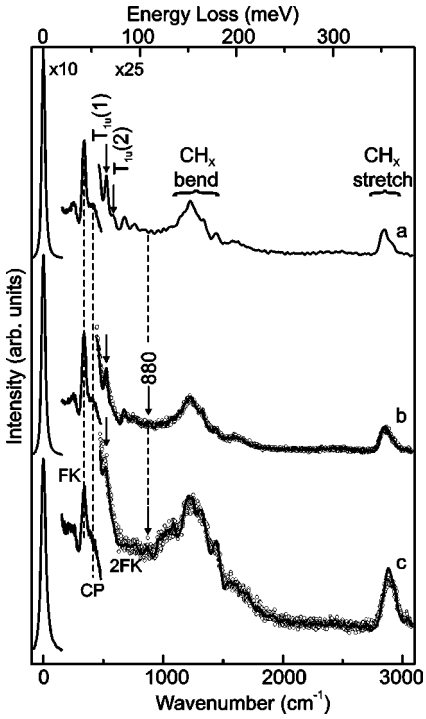

FIG. 8. HREEL spectra (primary beam energy 4.5 eV, incident angle 64° with respect to surface normal) of (a) 20 ML C_{60}/InP(001)-(2×4) 20 *L* exposed to atomic hydrogen; this surface after (b) 10^3 *L* molecular oxygen exposure; and (c) 2 h in air. Magnified (×25) parts of the spectra are deconvoluted, the raw spectra are depicted by open circles (see text). The C_{60} dipole active $T_{1u}(1,2)$ modes, substrate related carrier plasmon (CP), Fuchs-Kliewer phonon (FK, 2FK), and the mode at 880 cm^{-1} are marked (see text).

sponds to CH_x (possible values of x are 1,2,3) bending and stretching modes, respectively.[11,13,28] The intensity of C_{60} modes decreases. At 6 L exposure [curve (c)] the chemical modification is in an intermediate stage, and at about 20 L dosing [curve (d)] we reach a final stage. Further hydrogen dosing even up to 100 L (not shown) does not lead to notable spectral changes. The bands related to CH_x surface species are relatively strong, while the C_{60} peak intensities are damped, but still resolved.

The presented spectroscopic data indicate chemical modification of the C_{60} molecules, but there is not any evidence whether it is the hydrogenation or the cages cracking. The rest of the fullerene vibronic signature [Fig. 7(d)] can be related to the signal from C_{60}, attenuated by the products of the surface reaction, as well as to the vibrations of hydrofullerenes, which are not strongly affected by the hydrogen attachment. Also, the ultraviolet photoelectron spectroscopy data (not presented in this article) show relative decreasing of peaks corresponding to the π orbitals of fullerenes. This behavior can be related to the attenuation of the C_{60} response by the products of the cage destruction as in the former case, as well as to the destruction of the only π orbitals of C_{60} by the formation of hydrofullerenes (see also Ref. 25). The chemical composition of the reaction products does not evidently follow from the vibration or photoelectron spectroscopies. The molecule destruction by the atomic hydrogen was measured by a kind of mass-spectrometry technique and reported by Brühwiler *et al.*[26] The reaction of C_{60} with molecular hydrogen at elevated pressure and temperature leads to the molecule's decomposition, as follows from the complex studies of the reaction products.[27]

Fortunately, initially in our experiments the single domain molecular structure was formed. It is unlikely to destroy the order of these relatively big molecules by simple hydrogenation at low reagent dosing. Taking into account LEED data which show that the hexagonal pattern of the C_{60} multilayer disappears after 2 L atomic hydrogen dosing, we may conclude that the breaking up of the fullerene cages is caused by the surface reaction. The spectral behavior together with the structural study points to the following process: atomic hydrogen easily etches C−C bonds and cracks C_{60}, this reaction leads to the formation of a complex composition of hydrocarbons on the surface, which explains the broadness of the CH_x bands related to stretching and bending.

The intensities of the peaks related to the substrate are not changed by atomic hydrogen exposure. This indicates that the adsorbate thickness does not decrease and mostly higher hydrocarbons (which do not leave the surface) are the result of the process. The products of the C_{60} etching reaction form a film of hydrocarbon species on the surface and protect the underlying fullerene layers against further interaction with atomic hydrogen. This follows from the saturation of the surface reaction at atomic hydrogen dosing of about 20 L

and registering of the C_{60} spectral signature at the same time.

The chemical stability of the film resulting from the C_{60} cracking with respect to another reagent is illustrated in Fig. 8. Spectrum (a) corresponds to 20 ML of C_{60}/InP(001) [the same as in Fig. 7(d)], curve (b) was measured after 10^3 L oxygen exposure. Only a few weak features appear, among them, for example, a weak mode at 880 cm^{-1} (see Fig. 8), which is possibly related to the adsorption of molecular oxygen in a single bonded configuration.[28] Then the sample was exposed for 2 h in air and loaded back into the vacuum chamber. The increase of the CH_x vibration bands together with some decrease of substrate related peaks indicate the appearance of additional contaminations from air. Nevertheless, the C_{60} spectral signature is still present, which shows the stability of the fullerene underlayer also under atmospheric conditions. The detailed analysis of the spectroscopic data will be published elsewhere. These experiments prove the possibility of the formation of protective films for C_{60} structures without deposition of any other materials.

Our data can not be applied for a detailed analysis of surface or bulk contaminations of the C_{60} film. For electronic applications the penetration of molecular oxygen through the hydrocarbon layer requires additional investigations. For instance, the efficiency of the proposed treatment could be tested due to the strong influence of oxygen upon the conductivity of the fullerene film. In this contribution only the first experiments related to the protective properties of the hydrocarbon layer are included. We suggest, that the layer formed by the reaction of C_{60} with atomic hydrogen prevents or strongly attenuates diffusion of contaminants.

IV. CONCLUSION

The C_{60} fullerene growth on InP(001)-(2×4) was studied by surface sensitive UHV techniques. The vibronic spectra were measured by HREELS, the spectroscopic signature indicates weak molecule-substrate interaction resulting in 3D island growth at the initial stage of deposition. Further growth leads to a single domain molecular film formation, which was registered by LEED and STM. The well ordered structure is attractive for the design of electronic devices based on these materials.

In conjunction with possible applications, the stability of the growth mode with respect to surface defects of the substrate is an important property. Indium clusters are the most prevalent defects on InP and our data show that these clusters do not disturb the C_{60} growth in between. At the same time, our HREELS data reveal the changes of the surface carrier plasmon energy. Initially it increases due to the cluster formation (the shift is up to 110 cm^{-1}) and thus decreases after the molecule deposition (the shift is up to -55 cm^{-1}). The analysis of the plasmon behavior shows changes of the carrier concentration and depletion layer thickness after the surface treatment, which can strongly affect the charge flow in possible applications for electronic devices. The effect could be used for an improvement of semiconducting properties of thin C_{60} films, but needs to be investigated in more detail.

Properties of the molecular films exposed to atomic hydrogen were also studied. We found that a C_{60} film exposition to a relatively small amount of atomic hydrogen (a few minutes at a total pressure in the range of 10^{-7} Torr) destroys the top molecular layers, while further treatment does not change the surface any more. This observation points to the formation of a chemically stable hydrocarbon film on top of the molecular structure, which can serve as a protection against external contamination. This procedure could be used for the protection of fullerene related materials in electronic applications. A detailed analysis of these layers is planned.

ACKNOWLEDGMENTS

We are thankful to L. Carta-Abelmann and P. Scharff for providing us with C_{60} material for our experiments.

*Electronic address: Juergen.Schaefer@tu-ilmenau.de

[1] H. W. Kroto, J. R. Heath, S. C. O'Brien, R. F. Curl, and R. E. Smalley, Nature (London) **318**, 162 (1985).

[2] W. Krätschmer, L. D. Lamb, K. Fostiropoulos, and D. R. Huffman, Nature (London) **347**, 354 (1990).

[3] E. Frankevich, Y. Maruyama, and H. Ogata, Chem. Phys. Lett. **214**, 39 (1993).

[4] R. C. Haddon, A. S. Perel, R. C. Morris, T. T. M. Palstra, A. F. Hebard, and R. M. Fleming, Appl. Phys. Lett. **67**, 121 (1995).

[5] S. Kobayashi, T. Takenobu, S. Mori, A. Fujiwara, and Y. Iwasa, Appl. Phys. Lett. **82**, 4581 (2003).

[6] S. Kobayashi, T. Takenobu, S. Mori, A. Fujiwara, and Y. Iwasa, Sci. Technol. Adv. Mater. **4**, 371 (2003).

[7] A. R. Völkel, R. A. Street, and D. Knipp, Phys. Rev. B **66**, 195336 (2002).

[8] Y. S. Yang, S. H. Kim, J.-I. Lee, H. Y. Chu, L.-M. Do, H. Lee, J. Oh, T. Zyung, M. K. Ryu, and M. S. Yang, Appl. Phys. Lett. **80**, 1595 (2002).

[9] Q. Xue, Y. Ling, T. Ogino, T. Sakata, Y. Hasegawa, T. Hashizume, H. Shinohara, and T. Sakurai, Thin Solid Films **281**, 618 (1996).

[10] S. Suto, K. Sakamoto, D. Kondo, T. Wakita, A. Kimura, A. Kakizaki, C.-W. Hu, and A. Kasuya, Surf. Sci. **438**, 242 (1999).

[11] J. Schmidt, M. R. C. Hunt, P. Miao, and R. Palmer, Phys. Rev. B **56**, 9918 (1997).

[12] P. Dumas, M. Gruyters, P. Rudolf, Y. He, L.-M. Yu, G. Gensterblum, R. Caudano, and Y. J. Chabal, Surf. Sci. **368**, 330 (1996).

[13] M. R. C. Hunt, J. Schmidt, and R. E. Palmer, Phys. Rev. B **60**, 5927 (1999).

[14] Y. Chao, K. Svensson, D. Radosavkić, V. Dhanak, L. Ŝiller, and M. Hunt, Phys. Rev. B **64**, 235331 (2001).

[15] I. M. Dmitruk, N. L. Dmitruk, E. V. B. (Golovataya-Dzhymbeeva), J. G. Bañuelos, A. Esparza, and J. M. Saniger, Carbon **42**, 1089 (2004).

[16] P. A. Heiney, J. E. Fischer, A. R. McGhie, W. J. Romanow, A. M. Denenstein, J. P. McCauley, Jr., A. B. Smith, III, and D. E. Cox,

Phys. Rev. Lett. **66**, 2911 (1991).
[17] W. G. Schmidt, F. Bechstedt, N. Esser, M. Pristovsek, C. Schultz, and W. Richter, Phys. Rev. B **57**, 14 596 (1998).
[18] W. G. Schmidt, N. Esser, A. M. Frisch, P. Vogt, J. Bernholc, F. Bechstedt, M. Zorn, T. Hannappel, S. Visbeck, F. Willig, and W. Richter, Phys. Rev. B **61**, R16 335 (2000).
[19] C. D. MacPherson, R. A. Wolkow, C. E. J. Mitchell, and A. McLean, Phys. Rev. Lett. **77**, 691 (1996).
[20] F. Stietz, T. Allinger, V. Polyakov, J. Woll, A. Goldmann, W. Erfurth, G. J. Lapeyre, and J. A. Schaefer, Appl. Surf. Sci. **104**, 169 (1996).
[21] Y. Chao, K. Svensson, D. Radosavkić, V. Dhanak, M. R. C. Hunt, and L. Ŝiller, Phys. Rev. B **66**, 075323 (2002).
[22] D. Pahlke, J. Kinsky, C. Schultz, M. Pristovsek, M. Zorn, N. Esser, and W. Richter, Phys. Rev. B **56**, R1661 (1997).
[23] J. A. Schaefer, Physica B **170**, 45 (1991).
[24] K. Horiuchi, K. Nakada, S. Uchino, S. Hashii, A. Hashimoto, N. Aoki, Y. Ochiai, and M. Shimizu, Appl. Phys. Lett. **81**, 1911 (2002).
[25] T. R. Ohno, C. Gu, J. H. Weaver, L. P. F. Chibante, and R. E. Smalley, Phys. Rev. B **47**, 13 848 (1993).
[26] P. A. Brühwiler, S. Andersson, M. Dippel, N. Mårtensson, P. A. Demirev, and B. U. Sundqvist, Chem. Phys. Lett. **214**, 45 (1993).
[27] A. V. Talyzin, Y. M. Shulga, and A. Jacob, Appl. Phys. A: Mater. Sci. Process. **78**, 1005 (2004).
[28] H. Ibach and D. L. Mills, *Electron Energy Loss Spectroscopy and Surface Vibrations* (Academic Press, New York, 1982).
[29] B. G. Frederick, G. L. Nyberg, and N. V. Richardson, J. Electron Spectrosc. Relat. Phenom. **64/65**, 825 (1993).
[30] D. Briggs and M. P. Seah, *Practical Surface Analysis* (Wiley, New York 1983), Vol. 1.
[31] Y. Caudano, A. Peremans, P. A. Thiry, P. Dumas, and A. Tadjeddine, Surf. Sci. **368**, 337 (1996).
[32] E. I. Altman and R. J. Colton, Phys. Rev. B **48**, 18 244 (1993).
[33] A. Peremans, Y. Caudano, P. A. Thiry, P. Dumas, W. Q. Zhang, A. L. Rille, and A. Tadjeddine, Phys. Rev. Lett. **78**, 2999 (1997).
[34] C. Silien, Y. Caudano, A. Peremans, and P. A. Thiry, Appl. Surf. Sci. **163-163**, 445 (2000).
[35] F. S. Tautz, M. Eremtchenko, J. A. Schaefer, M. Sokolowski, V. Shklower, and E. Umbach, Phys. Rev. B **65**, 125405 (2002).
[36] K. G. Tschersich and V. von Bonin, J. Appl. Phys. **84**, 4065 (1998).
[37] K.-A. Wang, A. M. Rao, P. C. Eklund, M. S. Dresselhaus, and G. Dresselhaus, Phys. Rev. B **48**, 11 375 (1993).
[38] H. Kuzmany, R. Winkler, and T. Pichler, J. Phys.: Condens. Matter **7**, 6601 (1995).
[39] J. L. Feldman, J. Q. Broughton, L. L. Boyer, D. E. Reich, and M. D. Kluge, Phys. Rev. B **46**, 12 731 (1992).
[40] T. Hara, J. Onoe, and K. Takeuchi, Phys. Rev. B **63**, 115412 (2001).
[41] A. Lucas, G. Gensterblum, J. J. Pireaux, P. A. Thiry, R. Caudano, J. P. Vigneron, P. Lambin, and W. Krätschmer, Phys. Rev. B **45**, 13 694 (1992).
[42] Z.-H. Dong, P. Zhou, J. M. Holden, P. C. Eklund, M. S. Dresselhaus, and G. Dresselhaus, Phys. Rev. B **48**, 2862 (1993).
[43] M. R. C. Hunt, S. Modesti, P. Rudolf, and R. E. Palmer, Phys. Rev. B **51**, 10 039 (1995).
[44] W. L. Yang *et al.*, Science **300**, 303 (2003).
[45] L.-L. Wang and H.-P. Cheng, Phys. Rev. B **69**, 045404 (2004).
[46] A. A. Lucas, J. Phys. Chem. Solids **53**, 1415 (1992).
[47] G. Gensterblum, J. J. Pireaux, P. A. Thiry, R. Caudano, P. Lambin, and A. A. Lucas, J. Electron Spectrosc. Relat. Phenom. **64/65**, 835 (1993).
[48] M. Shimomura, N. Sanada, Y. Fukuda, and P. J. Moller, Surf. Sci. **359**, L451 (1996).